Stochastics, Meta-population models

Meifang Li
13043390
University of Amsterdam
Amsterdam, the Netherlands

Yuhao Qian
13011456
University of Amsterdam
Amsterdam, the Netherlands

ABSTRACT

When studying epidemiology, we can build two types of models: one is the deterministic model and the other is the stochastic model. In long term, these two models may behave similarly but in short-term dynamics, they are not. Now in this assignment, we mainly focus on the stochastic models. We would use Gillespie's Algorithm to explore the five hallmarks of an event-driven SIR model in the first part and build a meta-population model in the second part.

1 INTRODUCTION

The SIR model is one of the simplest models to account for infectious diseases. This model was initially studied by Kermack and Mckendrick(1927), where they categorized hosts within a population as Susceptible(S), Infected(I), and Recovered(R) [1]. The transitions are from S to I classes and from I to R classes.

We have discussed the deterministic model in the last assignment and would further introduce the stochastic model this time. In the first part, we would generate a SIR discrete event model using Gillespie's direct algorithm and explore the five hallmarks of stochastic SIR dynamics: variability, negative co-variances, increased transients, stochastic resonance and extinctions. To demonstrate all these aspects, we start with stochastic SIR without demography, then add demography to analyze the first four hallmarks and finally add imports to explore the last hallmark–extinctions. We would also measure the first passage time in the extinctions to analyze the relationship between population size and first passage time.

In the second part, we would implement a simple meta-population model to study the spatial dynamics of spreading infection. We start with a stochastic meta-population model with two subpopulations and demonstrate the effect of coupling between the two populations. Then we produce a meta-population using more subpopulations and use different strengths of interactions between populations to explore the dynamics.

2 PROBLEM1: GILLESPIE'S DIRECT ALGORITHM

2.1 SIR Model and Its Variations

Before we implement event-driven stochasticity into the SIR model. We would like to reintroduce the SIR model and its variations. Firstly we start with SIR without demography. The system can be represented by three ODEs:

$$\frac{dX}{dt} = -\beta\frac{XY}{N} \tag{1}$$

$$\frac{dY}{dt} = \beta\frac{XY}{N} - \gamma Y \tag{2}$$

$$\frac{dZ}{dt} = \gamma Y \tag{3}$$

Table 1: Different events in event-driven model

Event	Rate	Result
Infection	$\beta XY/N$	$X \to X-1, Y \to Y+1$
Recovery	γY	$Y \to Y-1, Z \to Z+1$
Birth	μN	$X \to X+1$
Death susceptible	μX	$X \to X-1$
Death infectious	μY	$Y \to Y-1$
Death recovered	μZ	$Z \to Z-1$

X, Y, Z is the number of the people who are susceptible, infectious, or recovered. The total population is $N = X + Y + Z$. The parameter β is the transmission rate or infection rate while γ represents the recovery rate.

Then we introduce natural birth rate ν and death rate μ into the SIR model. We assume that $\nu = \mu$ so the population is still closed. The standard SIR model becomes:

$$\frac{dX}{dt} = \nu N - \beta\frac{XY}{N} - \mu X \tag{4}$$

$$\frac{dY}{dt} = \beta\frac{XY}{N} - \gamma Y - \mu Y \tag{5}$$

$$\frac{dZ}{dt} = \gamma Y - \mu Z \tag{6}$$

Pathogens are likely to go through stochastic extinction during dynamics. To reduce the risk of pathogen fade-out, we would like to assume that there is a population-dependent external force ϵ that can cause new infectious cases.

$$\frac{dX}{dt} = \nu N - \beta\frac{XY}{N} - \epsilon X - \mu X \tag{7}$$

$$\frac{dY}{dt} = \beta\frac{XY}{N} + \epsilon X - \gamma Y - \mu Y \tag{8}$$

$$\frac{dZ}{dt} = \gamma Y - \mu Z \tag{9}$$

2.2 Gillespie's Direct Algorithm

Now we can implement an event-driven stochastic SIR model. In this model, we are supposed to consider each event separately. There are now six possible events that can occur; each can affect the number of relative classes by one. Details are shown in Table 1.

Gillespie's Direct Method is one of the most famous ways of implementing an event-driven stochastic SIR model. The following steps can explain *Gillespie's Direct Method*:

(1) All possible events are labelled as $E_1, ..., E_n$.
(2) The probability of each event occurs is $R_1, ..., R_n$.
(3) The total rate is $R_{total} = \sum_{m=1}^{n} R_m$.
(4) Generate a random number and the time until next event is $\delta t = \frac{-1}{R_{total}} log(RAND_1)$.

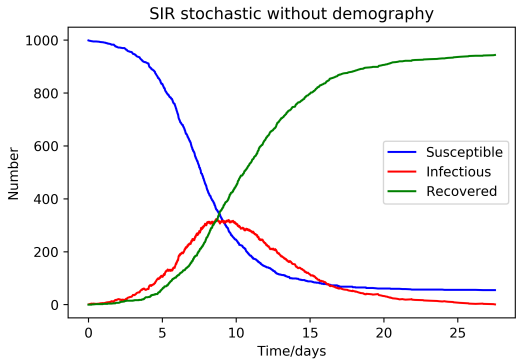

Figure 1: Stochastic SIR model without demography. The initial condition is $(S, I, R) = (999, 1, 0)$, with $\beta = 1perday, 1/\gamma = 3days$

(5) Generate a new random number, the next event is $P = RAND_2 \times R_{total}$.
(6) Event P occurs if :

$$\sum_{m=1}^{P-1} R_m < P \leq \sum_{m=1}^{P} R_m.$$

(7) $t \longrightarrow t + \delta t$, time is updated and event P occurred.
(8) Return back to step (2).

2.3 Five Hallmarks

2.3.1 Variability. The SIR models we mentioned in assignment1 are deterministic, which means the same initial condition would always have the same result. In the real world, it is impossible for us to predict the exact same result even if the situation keeps unchanged. Different simulations in the stochastic model could have different outcomes. The property can be revealed if we run the stochastic simulation several times. We firstly ran the Naive SIR without demography (Figure 1) and found that the curves were not as smooth as those in deterministic SIR model. This was because in event-driven models each possible event affect the number by one. In Figure 2 we obtained nine different simulations of the SIR model with demography. We ran this model for 200 days and noticed that some simulations even stopped at early stages. These different infectious curves showed the variability of the stochastic model.

2.3.2 Negative Covariance. As we can see in Figure 3, the number of susceptible and infectious seemed to have opposite trajectories roughly after 60 days. This phenomenon was more explicit in Figure 4. While the infectious curve peaked at the local maximum, the susceptible curve was near its local minimum. When the number of infectious climbed up during the first 60 days, the susceptible class already peaked once and decreased a large number of cases. By using *numpy.cov*, we obtained the covariance matrix of susceptible class and infectious class:
$\begin{bmatrix} 6163.00 & -279.68 \\ -279.68 & 519.82 \end{bmatrix}$. The number on the counter diagonal is the covariance we want but this covariance matrix was only one result of a certain simulation. So we ran the simulation for 10 times

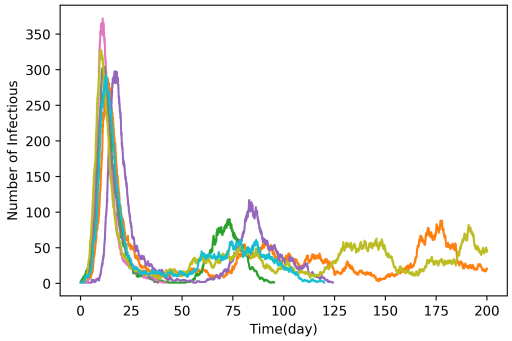

Figure 2: Various results of nine simulations with same initial condition in stochastic SIR with demography. The initial condition is $(S, I, R) = (999, 1, 0)$, with $\beta = 1perday, 1/\gamma = 3days, \mu = 1/60$

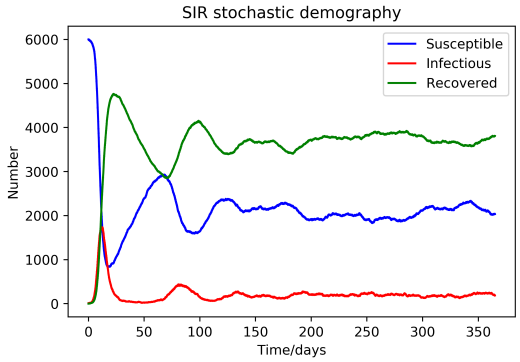

Figure 3: Stochastic SIR with demography. The initial condition is $(S, I, R) = (6000, 10, 0)$, with $\beta = 1perday, 1/\gamma = 3days, \mu = 1/60$

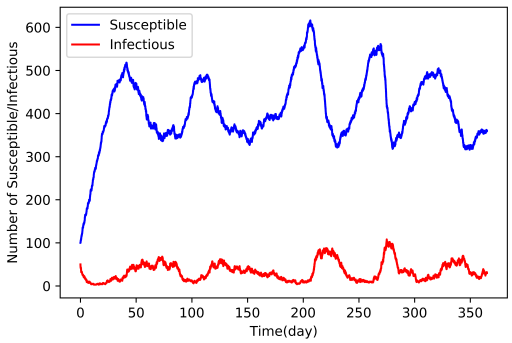

Figure 4: The negative covariance between susceptible and infectious. The initial condition is $(S, I, R) = (100, 50, 1000)$, with $\beta = 1perday, 1/\gamma = 3days, \mu = 1/60$

and got the average covariance -703.13. The negative covariance meant these two classes have opposite trends in general.

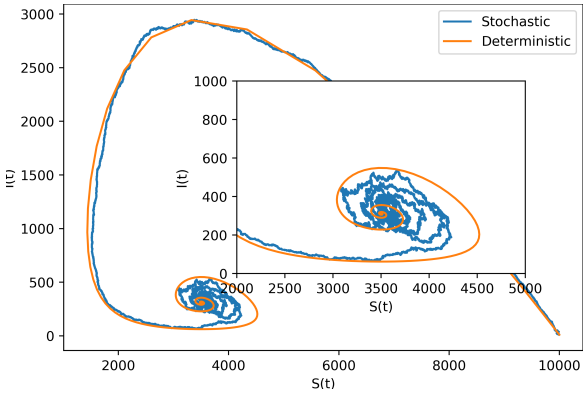

Figure 5: The trajectory of susceptible and infectious class. The initial condition is $(S, I, R) = (10000, 10, 0)$, with $\beta = 1perday, 1/\gamma = 3days, \mu = 1/60$

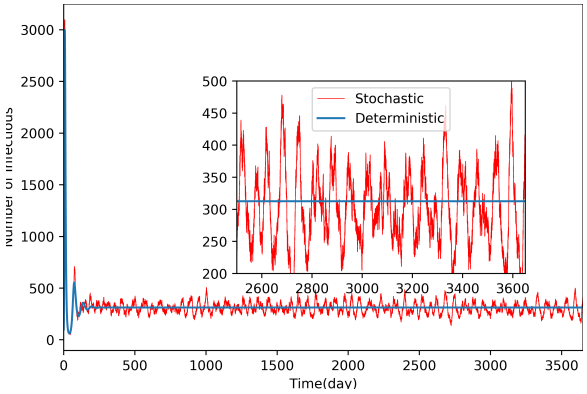

Figure 6: Transient dynamics. The initial condition is $(S, I, R) = (10000, 10, 0)$, with $\beta = 1perday, 1/\gamma = 3days, \mu = 1/60$.

2.3.3 Increased Transients. In the deterministic SIR model, we plotted a phase space diagram to reveal the dynamic property. We can do a similar thing to the stochastic SIR model. Figure 5 showed the trajectory of susceptible and infectious class. We plotted both the deterministic model and the stochastic model in the same plot. The deterministic curve converged to equilibrium quickly while the stochastic curve perturbed near-equilibrium point, as shown in the inset plot of Figure 5. When far from endemic equilibrium, the deterministic model acted as a strong attractor, so the behavior of the stochastic model is similar to the deterministic model.

2.3.4 Stochastic Resonance. The deterministic SIR model will decay approaching endemic equilibrium, while the stochastic model will oscillate due to its transient-like dynamics. It is because that SIR equilibrium is weakly stable and its oscillation near-equilibrium could easily be triggered by noise, assumed that stochasticity is a kind of noise. Figure 6 could explain stochastic resonance. The deterministic model(blue curve) declined quickly and then remained steady. However, the stochastic model(red curve), after similar behavior as the deterministic model at an early stage, oscillated constantly near deterministic equilibrium.

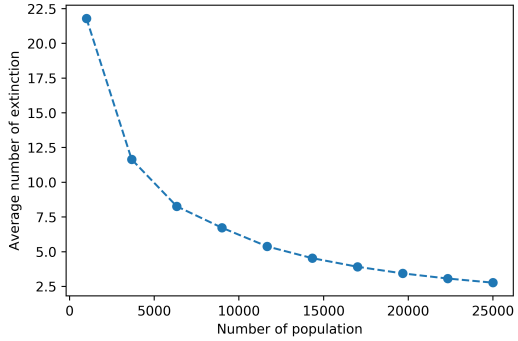

Figure 7: The average number of extinctions per year of SIR model with demography and external import, which has 25 different population sizes. The average number was obtained by 10 simulations at one population size. The simulations started near deterministic equilibrium $(S, I, R) = (0.05N, 0.05N, 0.9N)$, with $\beta = 1perday, \gamma = 2/3, \mu = 1/60$, import rate $\epsilon = 0.02\sqrt{N}peryear$.

2.3.5 Extinctions. The event-driven model is integer-valued because each possible event affects the number by one. So the number of infectious people can drop to zero in some cases, especially when the population size is small. To decrease the risk of permanent extinction, we would import external pathogens. We assumed there is an external force that could cause one susceptible individual to get infected:

$$X \longrightarrow X - 1, Y \longrightarrow Y + 1.$$

The rate of this infection force is $\epsilon(N)X$. In human populations, this force of infection is estimated scaling with the square root of the total population size. In our experiment the import rate is $\epsilon = 0.02\sqrt{N}peryear$.

As we mentioned, the risk of extinction will reduce as the increase in the population size. The smallest population size that will not undergo extinction is defined as *Critical Community Size (CCS)*. One way to measure this kind of persistence is to calculate the *First Passage Time*, which is to start the stochastic simulation near deterministic equilibrium and calculate the average time until the population of infectious get first extinction.

Figure 7 and Figure 8 showed our experimental results. We assumed initial condition $(S, I, R) = (0.05N, 0.05N, 0.9N)$ is not far from the deterministic equilibrium and operated simulations of each population size for 10 times. It was clear that the average number of annual extinctions decreased as the population N increased. Meanwhile, the *first passage time* increased and the increasing ratio became slower. It is because a pathogen gets harder to extinct in a large population if the transmission rate and recovery rate remain unchanged.

Besides, we ran the simulation at a relatively large population size and tried to figure out the Critical Community Size. Unfortunately, in Figure 9 our model still experienced one extinction after quite a long time. So the CCS here should over 200,000 for a extinction-free state.

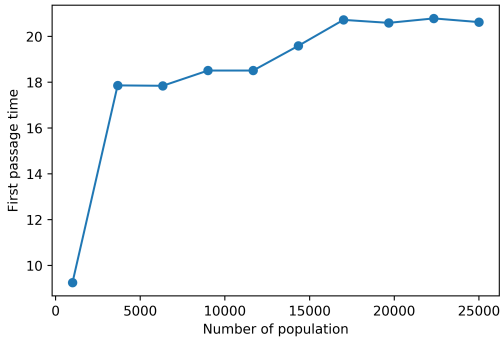

Figure 8: First passage time of SIR model with demography and external import. The initial condition is $(S, I, R) = (0.05N, 0.05N, 0.9N)$, with $\beta = 1perday, \gamma = 2/3, \mu = 1/60$, import rate $\epsilon = 0.02\sqrt{N}peryear$.

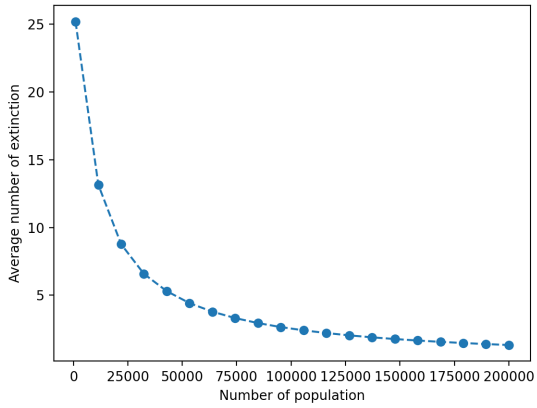

Figure 9: Trial to figure out the Critical Community Size. The simulations started near deterministic equilibrium $(S, I, R) = (0.05N, 0.05N, 0.9N)$, with $\beta = 1perday, \gamma = 2/3, \mu = 1/60$, import rate $\epsilon = 0.02\sqrt{N}peryear$.

3 PROBLEM2:META-POPULATION MODEL

In this section, we take the local nature of spatial transmission into account and introduce the meta-population model which is one of the simplest spatial models. We mainly analyze the effect of coupling between two populations and measure the lag between the peak of two populations with the different relative strength of transmission. Then we further absorb more subpopulations into meta-population model and use the different strength of interactions between populations to analyze the dynamics.

3.1 Coupling Two Populations

We start by implementing a simple meta-population model to study the spatial dynamics of spreading infection and analyze the relationship between the relative strength of transmission and the delay of the epidemic peak between two populations.

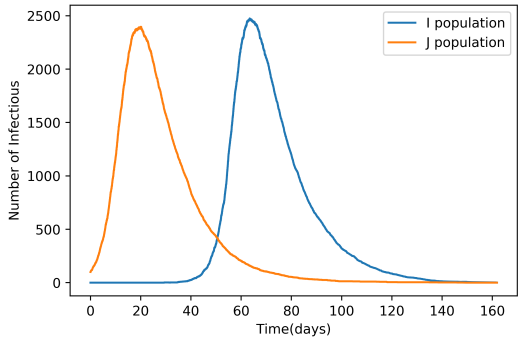

Figure 10: The effect of coupling between two populations, $X_i = 5000, Y_i = 0, Z_i = 0; X_j = 4900, Y_j = 100, Z_j = 0, \beta = 0.3571perday, 1/\gamma = 14days, \rho_{ii} = 1, \rho_{ij} = 0.8, \rho_{ji} = 0$

3.1.1 Meta-population Model. The concept of the meta-population is to subdivide the entire population into distinct subpopulations. Each subpopulation has independent dynamics and a limited form of interaction with each other. Assuming that there are n subpopulations and (X_i, Y_i, Z_i) are the number of susceptible, infectious and recovered individuals in subpopulation i. Likewise, $N_i = X_i + Y_i + Z_i$ is the total number of individuals in subpopulation i and $N = \sum_{i=1}^{n} N_i$ is the total population size. Then we could model interaction purely due to an additional force of infection λ_i and get

$$\frac{dX_i}{dt} = \nu_i N_i - \lambda_i X_i - \mu_i X_i \tag{10}$$

$$\frac{dY_i}{dt} = \lambda_i X_i - \gamma_i Y_i - \mu_i Y_i \tag{11}$$

This force of infection is the relation between force of infection in subpopulation i and the number of infectious individuals in subpopulation j, thus λ_i could be denoted as a weighted sum over prevalence in all populations as below

$$\lambda_i = \beta_i \sum_{j=1}^{n} \rho_{ij} \frac{Y_i}{N_i} \tag{12}$$

where ρ_{ij} is the relative strength of transmission to subpopulation i from subpopulation j.

3.1.2 Method and Discussion. We assumed that there were two large, fully susceptible subpopulations of the same size with $\rho_{ii} = 1, \rho_{ij} < 1$ and $\rho_{ji} = 0$ and ignore demography, which means that we introduce infection in subpopulation j and only couple from j to i to simplify the relative weak coupling. Then we take the coupling event into Gillespie's direct algorithm and generate the metapopulation model with an event-driven stochastic model of two subpopulations.

As shown in Figure10, we can see that there is a significant delay of the epidemic peak in subpopulation i and the lag time is 43.39 days. This may due to the fact that the susceptible of subpopulation i could be infected after enough time and chances of interactions with the infectious of subpopulation j , though the pathogen may eventually spread when ρ_{ij} is large enough. Additionally, we explored the effect of different coupling ρ_{ij} on the dynamics of the

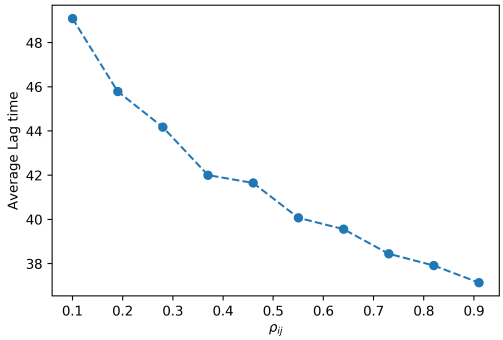

Figure 11: Average lag time of coupling between two populations with different ρ_{ij},$X_i = 5000, Y_i = 0, Z_i = 0; X_j = 4900, Y_j = 100, Z_j = 0, \beta = 0.3571 perday, 1/\gamma = 14 days, \rho_{ii} = 1, \rho_{ji} = 0$

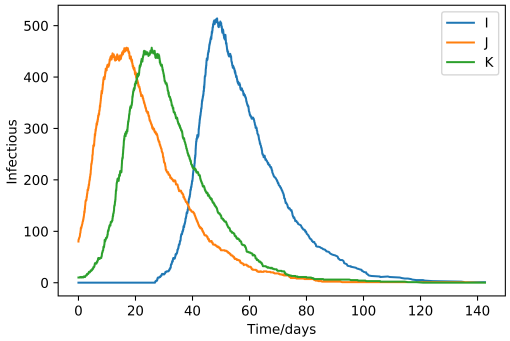

Figure 12: The effect of coupling between three populations, $X_i = 1000, Y_i = 0, Z_i = 0; X_j = 900, Y_j = 80, Z_j = 20, ; X_k = 990, Y_k = 10, Z_k = 0, \beta = 1/3 perday, 1/\gamma = 14 days, \rho_{ij} = 0.5, \rho_{jk} = 0.5, \rho_{ki} = 0.5$

epidemic in subpopulation i. We measured the average lag time of 20 runs between the peak of the epidemic in subpopulation j and the subsequent peak in subpopulation i. We can see from Figure11 that the delay between the peaks showed a dramatic decline as the coupling ρ_{ij} increased. Along with the coupling ρ_{ij} rising, the interactions between two subpopulations enhanced, thus the epidemic of subpopulation i arrived early and the delay dropped significantly.

3.2 Coupling Multiple Populations

In this part, We take more subpopulations into the meta-population model and explore the dynamics using the different strength of interactions between populations.

3.2.1 Method and Discussion. We took into account three large, fully susceptible subpopulations of the same size with $\rho_{ii} = 1$,$\rho_{ij} < 1$,$\rho_{jk} < 1$,$\rho_{ki} < 1$ and ignored demography, which meaned that we introduced infection in subpopulation j and subpopulation k and only coupled from j to i,from k to j and from i to k to analyze the dynamics. The steps of coupling three subpopulations that we took to generate the metapopulation model with Gillespie's direct algorithm were basically the same as coupling two subpopulations.

As shown in Figure12, we can see that the subpopulation j peaked first, followed by subpopulation k and finally subpopulation i. The initial infectious number of j was largest among the three subpopulations and it was also influenced by coupling from k to j, thus the pathogen would invade quickly and trigger an epidemic first in j. Although the coupling rates were the same between any two subpopulations, the subpopulation i showed the latest epidemic peak mainly because there were no infectious individuals in the first place. We also explored the effect of different coupling ρ_{ij} on the dynamics of the epidemic in subpopulation i. We measured the average peak time of 10 runs of the epidemic peak in subpopulation i. We can see from Figure13 that the time of peak declined significantly as the coupling ρ_{ij} increased. Intuitively, this may also due to the enhancing interactions that make the pathogen spread more easily when the coupling ρ_{ij} was larger.

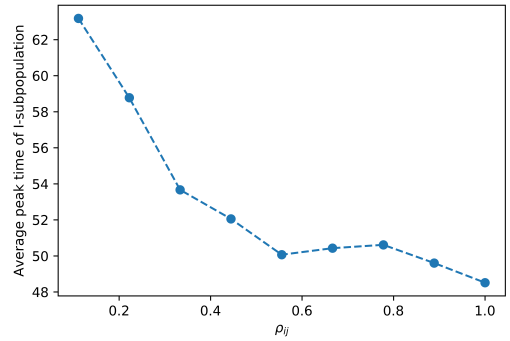

Figure 13: Average peak time of I population when coupling between three populations with different ρ_{ij}, $X_i = 1000, Y_i = 0, Z_i = 0; X_j = 900, Y_j = 80, Z_j = 20, ; X_k = 990, Y_k = 10, Z_k = 0, \beta = 1/3 perday, 1/\gamma = 14 days, \rho_{jk} = 0.5, \rho_{ki} = 0.5$

4 CONCLUSION

We first implemented event-driven stochasticity into the SIR model and analyzed the five hallmarks of stochastic SIR dynamics. Different simulations could have different outcomes, which showed variability. The number of susceptible and infectious showed opposite trends in the stochastic model, which meant these two classes have negative covariance. The stochastic model also behaved a transient-like return to its deterministic attractor when far from its equilibrium. When approaching equilibrium in decaying epidemics, the stochastic model dynamics would oscillate around the normal endemic prevalence. There were extinctions due to probability in this integer-valued stochastic model. With external imports, we found that the average number of annual extinctions decreased and the first passage time increased as population size increased.

As for the meta-population model, we noticed a significant delay of the epidemic peak between the two subpopulations, and the average lag time between the peaks declined as the relative strength of transmission increased. When coupling more subpopulations,

we obtained the fact that the average peak time of one in three subpopulations declines as the coupling interaction grew.

REFERENCES

[1] Matt J. Keeling and Pejman Rohani. 2007. *Modelling Infectious Diseases in Humans and Animals.* Princeton University Press.